ChemComm

COMMUNICATION

View Article Online
View Journal | View Issue

Cite this: *Chem. Commun.*, 2024, **60**, 12888

Received 27th August 2024,
Accepted 9th October 2024

DOI: 10.1039/d4cc04375h

rsc.li/chemcomm

Modelling and analysis of polarisation characteristics in lithium insertion electrodes considering charge transfer and contact resistances†

Kingo Ariyoshi * and Yuma Nagashima

The polarisation behaviour of $Li[Li_{0.1}Al_{0.1}Mn_{1.8}]O_4$ (LAMO) electrodes is influenced by charge transfer resistance (R_{ct}) and contact resistance (R_{cont}). In this study, using symmetric LAMO/LAMO cells, we find that polarisation curves shift from exponential (Tafel-like) to linear (Ohm's law-like) as R_{ct} decreases relative to R_{cont}, particularly at lower temperatures and higher frequencies. A new polarisation equation, based on an equivalent circuit model, explains the transition from exponential to linear polarisation curves observed in experiments. Our results indicate that reducing R_{cont} is more crucial than R_{ct} for improving electrode power capability.

The power capability of lithium-ion batteries (LIBs) is determined by the polarisation behaviour of the lithium insertion electrodes used as positive and negative electrodes. Electrochemical impedance spectroscopy (EIS) is most often used to analyse the reaction kinetics of lithium insertion electrodes,[1–5] as it allows the quantitative evaluation of the resistance components of the electrodes, such as charge transfer and contact resistances. However, because a linear relationship does not exist between the overpotential and current in electrochemical reactions, the polarisation behaviour of the electrode cannot be simply predicted from Ohm's law, assuming a linear response, even if the values of each resistance component obtained by EIS are identified. According to the electrochemical kinetic theory, the polarisation characteristic obeys the Tafel (more rigorously Butler–Volmer) equation; therefore, the current response should exhibit an exponential dependence on the overpotential. However, when steady-state polarisation measurements were performed for lithium insertion electrodes, a linear relationship between the applied voltage and current response was frequently observed.[6,7] In this study, to provide a reasonable explanation for the discrepancy between the polarisation behaviours—exponential relationship predicted by electrochemical theory *versus* linear relationship observed in actual lithium insertion electrodes—we developed a polarisation equation based on the equivalent circuit model determined from EIS measurements using symmetric cells.

As shown in Fig. 1a, the equivalent circuit of the lithium insertion electrodes comprising a series connection of the

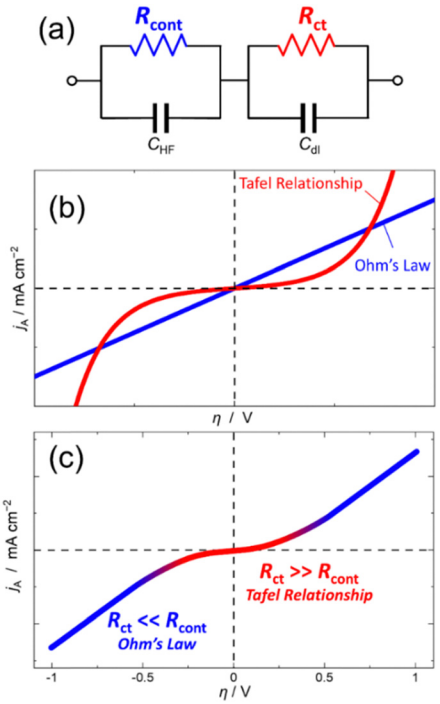

Fig. 1 (a) An equivalent circuit of lithium insertion electrodes comprising contact resistance (R_{cont}) and charge transfer resistance (R_{ct}) connected in series. (b) Current *versus* overvoltage relationship based on Ohm's law (blue) and Tafel equation (red). (c) Polarisation curve of lithium insertion electrodes calculated from eqn (1) based on the equivalent circuit of (a).

Department of Chemistry and Bioengineering, Graduate School of Engineering, Osaka Metropolitan University, 3-3-138 Sugimoto, Sumiyoshi, Osaka 558-8585, Japan. E-mail: ariyoshi@omu.ac.jp

† Electronic supplementary information (ESI) available: Experimental section; derivation of the polarisation equation of lithium insertion electrodes; XRD pattern of LAMO; charge–discharge profiles of a diluted-LAMO electrode; charge–discharge profiles of a symmetric cell; polarisation measurements of a symmetric cell; steady-state polarisation curves of a symmetric cell. See DOI: https://doi.org/10.1039/d4cc04375h

charge transfer resistance (R_{ct}) caused by the lithium insertion reaction and the contact resistance (R_{cont}) caused by the electron transfer between the electrode and current collector.[8–10] The overvoltage required for each process can be calculated by the Tafel equation for the activation overvoltage due to the charge transfer reaction (η_{ct}), and the Ohm's law for the resistance overvoltage due to the contact resistance (η_{cont}) (Fig. 1b). Therefore, the following polarisation equation for the lithium insertion electrode is obtained (see ESI† for derivation of the equation).

$$\eta = \frac{RT}{\alpha nF}\ln\left(\frac{nFR_{ct}}{RT}\times j\right) + R_{cont}\times j \qquad (1)$$

To depict the polarization curve, total current was obtained by sum of the cathodic and anodic currents calculated from eqn (1). The polarisation curve (Fig. 1c) can be divided into two regions: an exponential relationship similar to the Tafel relation at a small overvoltage, and a linear relationship similar to Ohm's law at a large overvoltage. When η_{ct} is much larger than η_{cont} at low current density, η is virtually equal to η_{ct}. Consequently, the polarisation curve follows Tafel's law. Conversely, when η_{ct} is significantly smaller than η_{cont} at high current density, η approaches to η_{cont} with increasing the current density. As such, the shape of the polarisation curve changes with the overpotential because the overpotential dependences of the two types of resistances comprising the equivalent circuit of the lithium insertion electrode are different.

$Li[Li_{0.1}Al_{0.1}Mn_{1.8}]O_4$ (LAMO) has a spinel structure (Fig. S1, ESI†) that was used as the active material. The electrochemical behaviour of the LAMO was examined using diluted-LAMO electrodes[11–13] *via* constant-current charge–discharge measurements. Procedures of electrode preparation and cell fabrication can be found in the ESI.† The charge–discharge curves of the Li/LAMO cells (Fig. S2, ESI†) show an operating voltage of 4 V with 103 mA h g^{-1} of rechargeable capacity, which is similar to that reported previously.[14] A LAMO/LAMO symmetric cell comprising two identical diluted-LAMO electrodes with the same weight, thickness, and capacity exhibited the same reversible capacity of 103 mA h g^{-1} as that of the Li/LAMO cell (Fig. S3, ESI†).

Steady-state polarisation measurements of the LAMO/LAMO-symmetric cells were performed to investigate the polarisation behaviour of the LAMO electrode (Fig. 2a–c). For steady-state polarisation measurements, a sinusoidal voltage with large amplitude of 1000 mV was applied to the cell to measure the response current (see ESI† for experimental details).[6,7] At frequencies of 10 and 1.0 Hz, current profiles were sinusoidal in shape as the same as the applied voltage without any phase difference, while the current was distorted at frequency of 10 mHz especially in small overvoltage region. The maximum current density increased with the frequency. Steady-state polarisation curves were obtained by plotting the output current against the applied voltage (Fig. 2d–f). The shapes of the polarisation curves changed significantly depending on the frequency. At low frequency (10 mHz), the polarisation curve was distorted to an exponential relationship, although the

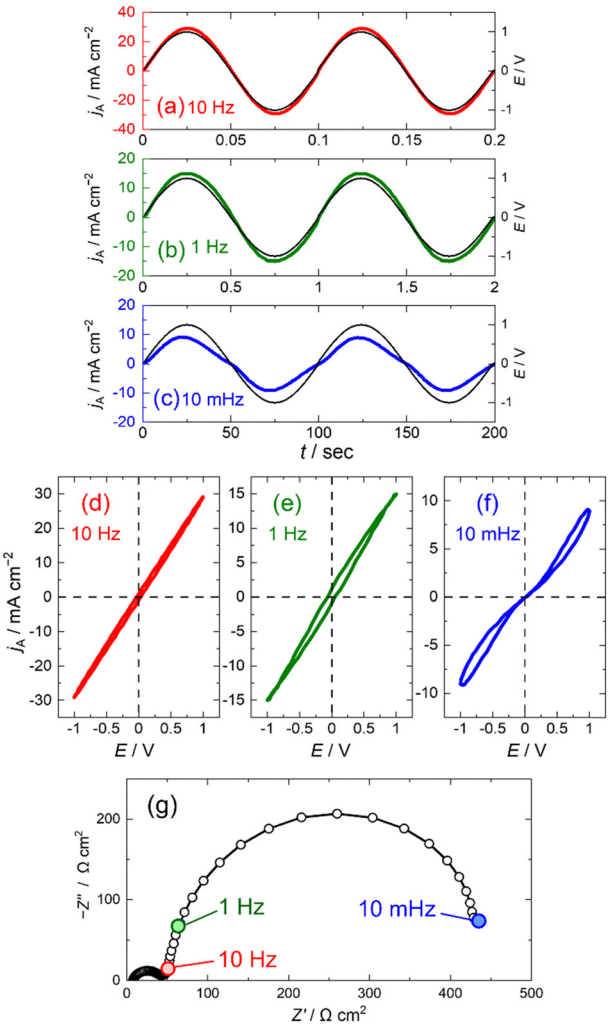

Fig. 2 (a)–(c) Applied voltage and output current for polarisation measurements; (d)–(f) steady-state polarisation curves of a LAMO/LAMO symmetric cell at −15 °C. The frequency of applied voltage was (a) and (d) 10 Hz, (b) and (e) 1 Hz and (c) and (f) 10 mHz. (g) The Nyquist plot of the LAMO/LAMO symmetric cell measured at −15 °C.

polarisation curves were linear at high frequencies of 1 and 10 Hz, indicating that the polarisation behaviour of the LAMO electrode is based on Tafel relationship and Ohm's law at low and high frequencies, respectively.

EIS measurements were performed on the LAMO/LAMO symmetric cell to investigate the frequency dependence of the polarisation curves (Fig. 2g). The Nyquist plot shows two semicircles attributed to contact resistance (R_{cont}) and charge transfer resistance (R_{ct}) for the high- and low-frequency arcs, respectively.[15–20] In the Nyquist plot, the impedance (Z) of 10 and 1.0 Hz were located at the end of the high-frequency arc, while the Z of 10 mHz at the end of the low-frequency arc, indicating that R_{ct} should be ignored in the polarisation measurements at 10 and 1.0 Hz, and the resistance of the LAMO electrodes is dominated by R_{cont} alone.

Consequently, the polarisation curves at 10 and 1 Hz were determined using Ohm's law, which resulted in a linear curve owing to the contribution of R_{cont}. However, at frequency at

10 mHz, the resistance of the LAMO electrode includes R_{ct} in addition to R_{cont}. Therefore, the polarisation behaviour at low frequency can be described by eqn (1), considering both R_{ct} and R_{cont}, results in a distorted polarisation curve with an exponential shape. These results indicate that to calculate the polarisation curves of lithium insertion electrodes, it is necessary to consider not only R_{ct} for the lithium insertion/extraction reaction but also R_{cont} originating from the electronic conduction between the active materials and the current collector.

Previous studies show that R_{ct} follows the Arrhenius relationship, wherein R_{ct} increases significantly as temperature decreases, whereas R_{cont} is almost constant regardless of the temperature.[9,21] Therefore, polarisation measurements at different temperatures enable the investigation of how the polarisation curves change with the ratio of the two resistances. In the steady-state polarisation curves measured at different temperatures of −15, −2, and 25 °C (Fig. S4, ESI†), the output current at 25 °C exhibits sinusoidal shape in spite of the large voltage of 1000 mV; however, it was distorted at −15 °C especially in the low overvoltage region.

The polarisation curves obtained by plotting the output current against the applied voltage exhibited different shapes depending on the temperature (Fig. 3a–c). Although the measured frequencies are different, this difference does not affect the shape of polarization curves (Fig. S5, ESI†). The curves at 25 and −2 °C showed linear relationship, whereas the curve at −15 °C showed an exponential relationship. This indicates that the polarisation curve of the lithium insertion electrodes changed from linear to exponential when the measurement temperature decreased. Such a change in the shape of the polarisation curves can occur when R_{ct} decreases as the temperature decreases.

To confirm that the curve shape was related to the resistance ratio R_{ct}/R_{cont}, the polarisation curves were fitted using eqn (1). By adjusting the values of R_{ct} and R_{cont}, the calculated polarisation curves (black lines) were well-fitted to the observed curves. At −15 °C, where the polarisation curve showed an exponential shape, the R_{ct} and R_{cont} were 400 and 80 Ω cm^2, respectively, and R_{ct} was 5 times larger than R_{cont}. Conversely, R_{ct} significantly decreased as the temperature increased. At −2 or 25 °C where the polarisation curve was linear, R_{ct} was two times larger or virtually the same as R_{cont}, respectively.

To verify the validity of R_{ct} and R_{cont} estimated by fitting the polarisation curves, EIS measurements were performed on the LAMO/LAMO symmetric cell at −15, −2, and 25 °C. (Fig. 3d–f). The size of the high-frequency arc attributed to the contact resistance was approximately constant regardless of the temperature, whereas the size of the low-frequency arc attributed to the charge-transfer resistance increased significantly with decreasing temperature. Comparing R_{ct} and R_{cont} at each temperature determined from the curve fitting and EIS (Table 1), R_{cont} showed a slight deviation owing to the solution resistance, but the R_{ct} values were approximately consistent. The good agreement between R_{ct} and R_{cont} determined by EIS and polarisation curve fitting proves that the polarisation equation developed in this study enables the prediction of the power capability of the lithium insertion electrodes and provides a rational explanation of the polarisation curves from a linear to exponential shape.

It has been reported that the temperature change of R_{ct} follows the Arrhenius equation.[8–10] Thus, by taking into account the temperature dependence of R_{ct}, the polarization equation is expressed by the following equation.

$$\log\left(\frac{1}{R_{ct}}\right) = A\exp\left(\frac{-E_a}{RT}\right)$$

However, in this paper, it is difficult to estimate Arrhenius parameters of the activation energy E_a and pre-exponential factor A due to the small number of measurement points at different temperatures. In previous reports,[8–10] R_{cont} has almost no temperature dependence, and the temperature dependence of R_{ct} follows the Arrhenius relationship. Consequently, by obtaining the Arrhenius parameters, it is possible to predict polarization behaviour over a wide temperature range with a single polarization equation, but it will be a research topic in the future.

As discussed above, the shape of polarisation curves of lithium insertion electrodes is determined by the ratio of R_{cont} and R_{ct}. The polarisation curve shows a linear relationship for $R_{ct} < R_{cont}$, whereas it has an exponential relationship for

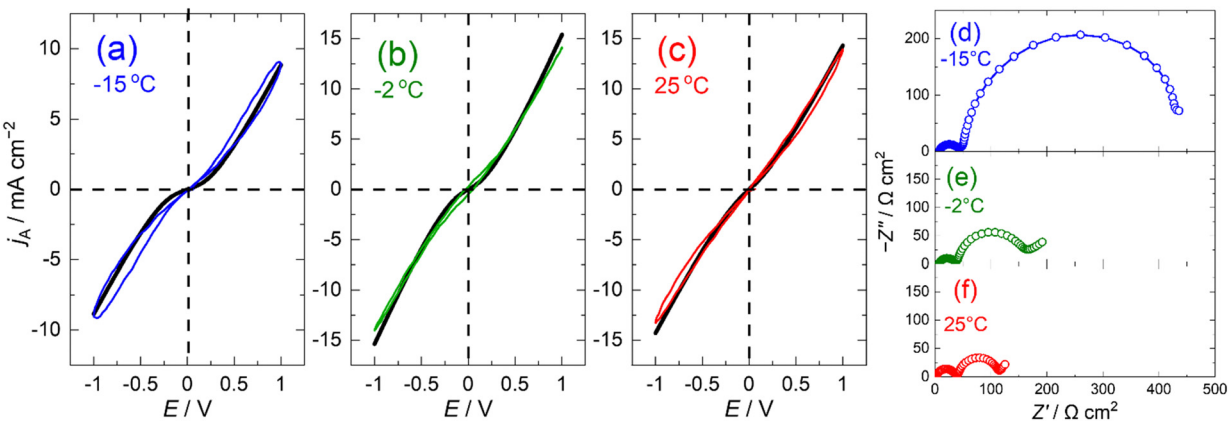

Fig. 3 (a)–(c) Steady-state polarisation curves and (d)–(f) Nyquist plots of the LAMO/LAMO symmetric cell at (a) and (d) −15, (b) and (e) −2 and (c) and (f) 25 °C. The frequency of applied voltage was (a) 10, (b) 100 and (c) 100 mHz.

Table 1 R_{ct} and R_{cont} of the LAMO/LAMO symmetric cell at −15, −2 and 25 °C determined from EIS measurements and polarisation-curve fitting. The unit of resistance values is Ω cm^2

Temp. (°C)		Impedance	Polarisation
−15	R_{ct}	400	400
	R_{cont}	50	80
−2	R_{ct}	125	100
	R_{cont}	40	60
25	R_{ct}	70	70
	R_{cont}	40	60

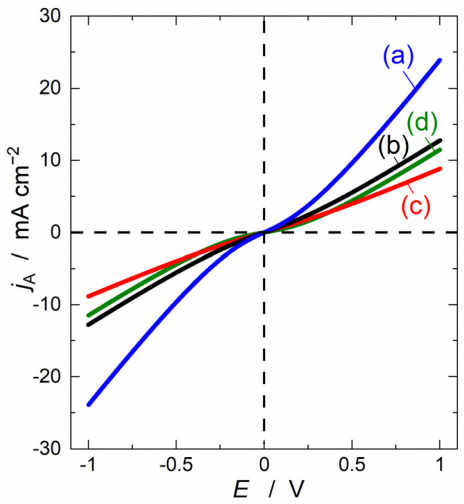

Fig. 4 Simulated polarisation curves of a lithium insertion electrode calculated from eqn (1) based on the equivalent circuit in Fig. 1a. Values of R_{ct} and R_{cont} are (a) 60 and 30, (b) 60 and 60, (c) 60 and 90 and (d) 180 and 60 Ω cm^2, respectively.

$R_{ct} > R_{cont}$. To clarify the impact of R_{ct} and R_{cont} on the power density of the lithium insertion electrodes, the polarisation curves were calculated based on eqn (1) for various ratios of R_{ct} to R_{cont}, as shown in Fig. 4. When R_{cont} decreased and R_{ct} remained constant, the output current varied significantly in the large-overvoltage region, which was associated with the change in the polarisation curves from linear to exponential. Conversely, no change in the output current was observed with varying R_{ct}. From these results, we can conclude that as R_{cont} decreases, the power capability of the electrodes improves dramatically. In other words, the power capability is significantly affected by R_{cont} rather than R_{ct}.

In summary, the polarisation behaviour of lithium insertion electrodes was investigated using a symmetric LAMO/LAMO cell, and the polarisation curve changed from linear to exponential depending on the temperature and frequency. The polarisation equation derived from an equivalent circuit model in which the charge transfer and contact resistances were connected in series was successfully used to reproduce the observed polarisation curves. The values of R_{ct} and R_{cont} estimated by fitting the polarisation curves are in good agreement with those obtained by EIS measurements. Therefore, the shape of the polarisation curve is determined by the ratio of R_{ct} and R_{cont}; $R_{ct} > R_{cont}$ leads to the distorted curve *versus* $R_{ct} < R_{cont}$ to linear curve. Furthermore, reducing R_{cont} rather than R_{ct} plays a more important role in increasing the power capability of the lithium insertion electrodes.

This work was supported by a grant from the GteX Program Japan (JPMJGX23S5) and the 2024 Osaka Metropolitan University (OMU) Strategic Research Promotion Project (Priority Research).

Data availability

The data supporting this article have been included as part of the ESI.†

Conflicts of interest

There are no conflicts to declare.

References

1 T. Osaka, D. Mukoyama and H. Nara, *J. Electrochem. Soc.*, 2015, **162**, A2529–A2537.
2 H. Nara, T. Yokoshima and T. Osaka, *Curr. Opin. Electrochem.*, 2020, **20**, 66–77.
3 K. Ariyoshi, Z. Siroma, A. Mineshige, M. Takeno, T. Fukutsuka, T. Abe and S. Uchida, *Electrochemistry*, 2022, **90**, 102007.
4 K. Ariyoshi, Z. Siroma, A. Mineshige, M. Takeno, T. Fukutsuka, T. Abe and S. Uchida, *Electrochemistry*, 2022, **90**, 102008.
5 K. Nakura, K. Ariyoshi, F. Ogaki, K. Takaoka and T. Ohzuku, *J. Electrochem. Soc.*, 2014, **161**, A841–A846.
6 T. Ohzuku, R. Yamato, T. Kawai and K. Ariyoshi, *J. Solid State Electrochem.*, 2007, **12**, 979–985.
7 K. Ariyoshi, Y. Maeda, T. Kawai and T. Ohzuku, *J. Electrochem. Soc.*, 2011, **158**, A281–A284.
8 H. Nara, D. Mukoyama, T. Yokoshima, T. Momma and T. Osaka, *J. Electrochem. Soc.*, 2016, **163**, A434–A441.
9 H. Nara, D. Mukoyama, R. Shimizu, T. Momma and T. Osaka, *J. Power Sources*, 2019, **409**, 139–147.
10 K. Ariyoshi, *Electrochemistry*, 2024, **92**, 37007.
11 K. Ariyoshi, S. Mizutani, T. Makino and Y. Yamada, *J. Electrochem. Soc.*, 2018, **165**, A3965–A3970.
12 K. Ariyoshi, J. Sugawa and S. Masuda, *J. Electrochem. Soc.*, 2020, **167**, 140517.
13 K. Ariyoshi, J. Sugawa and S. Masuda, *J. Power Sources*, 2021, **509**, 230349.
14 K. Ariyoshi, E. Iwata, M. Kuniyoshi, H. Wakabayashi and T. Ohzuku, *Electrochem. Solid-State Lett.*, 2006, **9**, A557–A560.
15 A. S. Keefe, S. Buteau, I. G. Hill and J. R. Dahn, *J. Electrochem. Soc.*, 2019, **166**, A3272–A3279.
16 K. Ariyoshi, S. Mizutani and Y. Yamada, *J. Power Sources*, 2019, **435**, 226810.
17 K. Ariyoshi, M. Tanimoto and Y. Yamada, *Electrochim. Acta*, 2020, **364**, 137292.
18 L. A. Middlemiss, A. J. R. Rennie, R. Sayers and A. R. West, *Energy Rep.*, 2020, **6**, 232–241.
19 M. Gaberščček, *Nat. Commun.*, 2021, **12**, 6513.
20 L. Stolz, M. Gaberščček, M. Winter and J. Kasnatscheew, *Chem. Mater.*, 2022, **34**, 10272–10278.
21 N. Ogihara, S. Kawauchi, C. Okuda, Y. Itou, Y. Takeuchi and Y. Ukyo, *J. Electrochem. Soc.*, 2012, **159**, A1034–A1039.